Ah receptor signaling controls the expression of cardiac development genes

Vinicius S. Carreira[1], Yunxia Fan[1], Qing Wang[1], Xiang Zhang[1], Hisaka Kurita[1], Chia-I Ko[1], Mindi Natichioni[2], Min Jiang[2], Sheryl Kock[2], Mario Medvedovic[1], Jack Rubinstein[2], and Alvaro Puga[1,*]

[1]Department of Environmental and Center for Environmental Genetics, and
[2]Department of Internal Medicine, Cardiology Division
University of Cincinnati College of Medicine, Cincinnati, Ohio 45267

Supplemental Material- List of Contents

1. Supplemental Materials and Methods

a. Animals and Treatments

All experiments were conducted using the highest standards of humane care in accordance with the NIH Guide for the Care and Use of Laboratory Animals and were approved by the University of Cincinnati Institutional Animal Care and Use Committee. C57BL/6J mice used in these experiments were originally purchased from the Jackson Labs and thereafter maintained in our colony. C57BL/6J mice were housed in a pathogen-free animal facility under a standard 12-hour light/12-hour dark cycle with *ad libitum* water and chow. $Ahr^{-/-}$ mice crossed for 7 generations into a C57BL/6J background were initially purchased from Jackson labs and thereafter maintained to date in our laboratory into the C57BL/6J genetic background (for about 14 years). On gestation day (GD) 7.5 pregnant $Ahr^{+/+}$ dams were treated by oral gavage with either corn oil (vehicle) or with TCDD (0.1, 0.5, 1, 2.5, 5, or 50 μg/kg of maternal weight) in corn oil vehicle, which was repeated on embryo days E9.5 and E11.5; $Ahr^{-/-}$ pregnant dams remained untreated throughout gestation. TCDD doses were specifically selected to include environmentally-relevant ranges and are within range of the reported mean human background body burdens for dioxin and dioxin-like compounds (PCDDs/PCDFs/PCBS) of approximately 9–13 ng TEQ/kg (DeVito et al. 1995).

b. Histology, Immunohistochemistry, and Microscopy

Following euthanasia, the *uteri* were harvested into chilled phosphate buffered saline (PBS). The number of embryos was counted and each embryo was dissected, blotted, and weighed. Following weight determination, each embryo was sectioned transversally at the level of the diaphragm for optimal fixative perfusion. Histological sections of the embryonic hearts

were obtained by transversal serial sectioning of the entire embryo thorax and collected on charged glass slides (Fisherbrand Superfrost Plus, Fisher Scientific).

For immunohistochemistry, rabbit polyclonal primary antibodies against AHR (SA-210 Enzo), NKX2-5 (Ab35842, Abcam), and Ki-67 (anti-rabbit, Millipore) were used at 1:200, 1:100, and 1:200 dilutions, respectively. The primary antibodies were probed with either a DAB kit (ImmunoCruz rabbit ABC Staining System, Santa Cruz) or fluorescently labeled secondary antibodies (AlexaFluor 488/594/680, Life Technologies). For DAB stains the sections were counter-stained with Harris hematoxylin (Sigma-Aldrich) as recommended by the DAB kit manufacturer, while for fluorescence analyses the nuclei were identified with DAPI present in the cover slip mounting medium (Vector Labs®). Macroscopic examinations and images were obtained using a dissection microscope (Leica MZ16FA equipped with a DFC4802 camera and Leica Application Suite).

Histomorphometry and microscopic images were obtained with a bright field microscope (Zeiss Axio Scope.A1) equipped with an AxioCam ERc5s and the Zen Blue Edition suite (Zeiss). Masson's trichrome histochemistry was performed as instructed by the manufacturer (ScyTek Laboratories). Quantification of fibrosis on Masson's trichrome-stained sections imaged at 40x were performed as described elsewhere (Teekakirikul et al. 2010). Immunostaining quantification was performed using the color deconvolution plugin and threshold functions of the ImageJ 1.47h (National Institutes of Health) on 15 non-overlapping high power field (40x) images per embryo (encompassing right and left atria, right and left ventricles, and interventricular septum). These images were used to determine the number of labeled nuclei versus the total number of nuclei, which was later factored in to yield the percentage of nuclei labeled (% positive index).

c. RNA.seq analysis

Following euthanasia of the dam, the uteri were immediately harvested and rinsed with sterile chilled phosphate buffered saline (PBS) and blotted dry. Embryos were dissected from the uterus and immediately transferred into RNA-Later (Ambion) where the hearts were excised. Each heart was microdissected into right atrium, left atrium, and ventricles with the assistance of a dissecting microscope. Individual samples were stored in 200 µL of RNA-Later at -80°C until RNA extraction. Total RNA was extracted with the RNeasy Mini Kit with Proteinase K and DNAse steps (QIAGEN).

All steps of library construction, cluster generation, and HiSeq (Illumina) sequencing were performed with biological triplicate samples by the Genomics Sequencing Core of the Department of Environmental Health, University of Cincinnati. Library construction was done with the TruSeq RNA sample preparation kit (Illumina) using 1 µg of total RNA, with RNA integrity number ≥ 7.0 as determined with an Agilent 2100 Bioanalyzer (Agilent Technologies) to purify poly-A–containing mRNA with oligo-dT–attached magnetic beads. The purified mRNA was enzymatically fragmented, with random hexamers primed for first and second strand cDNA synthesis, followed by purification using Agencourt AMPure XP beads (Beckman Coulter). Overhangs in the double-strand cDNA were blunt-ended by end repair and adenylated with a single A-nucleotide at the 3´ end to prevent self-ligation in the following ligation step. AMPure XP bead-purified fragments were ligated to sample-specific indexing adapters and enriched by 10 cycles of PCR using adapter-specific primers. A 1-µL aliquot of purified PCR product (from a total sequencing library of 30 µL) was analyzed in an Agilent bioanalyzer using a DNA 1000 chip to check DNA size (~ 260 bp) and yield. To quantify the library concentration for clustering, the library was diluted 1:100 in a buffer containing 10 mM Tris-HCl, pH 8.0, and

0.05% Tween 20, and analyzed by quantitative PCR (qPCR) with a KAPA Library Quantification kit (KapaBiosystems) using an ABI 9700HT real-time PCR machine (Applied Biosystems). Equal amounts of six individually indexed cDNA libraries were pooled for clustering in an Illumina cBot system flow cell at a concentration of 8 pM using Illumina's TruSeq SR Cluster Kit v3, and sequenced for 50 cycles using a TruSeq SBS kit on the Illumina HiSeq system. Each sample generated approximately 30 million sequence reads. Sequence reads were demultiplexed and exported to fastq files using CASAVA 1.8 software (Illumina). The reads were then aligned to the reference genome (mm10) using TopHat aligner. The counts of reads aligning to each gene's coding region were summarized using ShortRead and associated Bioconductor packages (GenomicFeatures, IRanges, GenomicRanges, Biostrings, Rsamtools) for manipulating and analysis of next-generation sequencing data and custom-written R programs.

Differential gene expression analysis between $Ahr^{+/+}$ and $Ahr^{-/-}$ embryos or between AHR ligand-exposed and naïve $Ahr^{+/+}$ embryos was performed separately at each of the three different developmental time points (E13.5, E15.5, and E18.5). Statistical analyses were performed to identify differentially expressed genes for each comparison using the negative-binomial model of read counts as implemented in the Bioconductor DESeq package. Significant genes were selected based on a false-discovery rate–adjusted p-value < 0.0001. We analyzed the RNA.seq data using Ingenuity Pathway Analysis (IPA; Ingenuity® Systems, http://www.ingenuity.com).

d. *Embryo (in utero) echocardiography*

At the gestation day corresponding to embryonic day (E) 15.5, three naïve (vehicle) $Ahr^{+/+}$, five AHR ligand exposed $Ahr^{-+/+}$, and five $Ahr^{-/-}$ pregnant dams were lightly sedated with isoflurane anesthesia on a heated pad and their lower abdomen shaved. In order to avoid imaging

the same embryo twice, the probe was placed on the far lower right flank of the abdomen and mechanically transitioned caudal to cranial while stopping to obtain B-mode (bright 2D image), M-mode (motion mode), color and Doppler images of each embryo's cardiac structure, the process was then repeated identically on the left side. Embryonic orientation, in order to determine right and left ventricle, was confirmed via scanning from top to bottom of each embryo and by using abdominal organs laterality. The *in utero* echocardiographic data was averaged for all the embryos in a litter and analyzed as the mean±SEM of the litters.

2. Supplemental Results

a. *Experimental design and gestational outcomes*

The experimental design, including the activation of AHR by ligand (TCDD) exposure, is illustrated in Supplemental Fig. 1A. Gestational AHR agonist exposure resulted in significant embryo body weight increase at E18.5 (wet and dry weights) while a decrease in body weight (dry only) was observed at E18.5 with AHR receptor ablation (Supplemental Fig. S1B and S1C). Maternal and embryo liver weights were measured as a proxy for ligand exposure, since accumulation and increase in liver weight is a well-documented effect of AHR agonist exposure (Besteman et al. 2007; Weinstein et al. 2008). Gestational AHR agonist exposure resulted in significant dose-dependent increases in liver weights in both dams (Supplemental Fig. S1D) and embryos (Supplemental Fig. S1E and S1F), corroborating embryo exposure to the AHR agonist. In contrast, $Ahr^{-/-}$ livers were significantly smaller than naïve $Ahr^{-+/+}$ dam livers, in agreement with the documented highly-penetrant portosystemic shunting phenotype associated with constitutional deletion of the AHR (Lahvis et al. 2000). AHR agonist exposure at the highest dose (i.e. 50 μg/kg) resulted in no statistically-significant changes to maternal heart, spleen, or

kidney weights (data not shown). Using the described exposure design, exposures at doses of 2.5 µg/kg and higher resulted in 100% perinatal lethality, occurring mostly within 48 hours of birth (Supplemental Fig. S1G). No statistically-significant reductions in the numbers of viable embryos (i.e. live at the time of sampling) were observed for either dose across time points, except for *Ahr*$^{-/-}$ litters (Supplemental Fig. S1H); the latter also being a documented effect of constitutional AHR ablation (Abbott et al. 1999). Macroscopic examination of embryos and stillbirths revealed a dose-dependent increased incidence of palatoschisis (cleft palate), an established teratogenic effect of this specific AHR agonist (TCDD), in embryos from dams who received doses of 2.5 µg/kg or higher. Palatoschisis was interpreted to be one of the contributing factors for the observed perinatal mortality in exposures at doses of 2.5 µg/kg and higher, but not all decedent pups were affected. A subset of pups from each treatment condition (up to and including the 1 µg/kg dose) was carried to PND30 and subsequently necropsied to assess the occurrence of overt terata, such as hydronephrosis and palatoschisis, except none was observed upon gross examination (data not shown).

3. Supplemental Tables

a. Supplemental Table S1

E15.5 Right Atrium - Differentially expressed genes					
Gene	**Naïve Ahr KO**		Gene	**Ahr WT + TCDD**	
	log ratio	p-value		log ratio	p-value
Hand1	-2.5758	7.23E-12	*Myl2*	-2.9375	4.03E-40
Myl2	-2.3784	1.36E-25	*Irx4*	-2.134	3.07E-32
Irx4	-2.285	8.35E-38	*Hopx*	-2.0144	2.61E-35
Hey2	-1.8987	1.09E-27	*Hand1*	-2.006	7.37E-08
Bves	-1.8381	3.48E-33	*Mycn*	-1.666	1.04E-15
Mycn	-1.6946	2.34E-16	*Hey2*	-1.5173	9.98E-19
Hopx	-1.6742	1.09E-28	*Bves*	-1.5016	1.13E-22
Gja1	-1.614	1.75E-28	*Gja1*	-1.2953	1.15E-18
Dio2	-1.5157	0.00019	*Cited1*	-1.0917	6.14E-06
Cited1	-1.2072	5.04E-11	*Dio2*	-0.8163	0.00628
Apln	-0.8293	0.00117	*Apln*	-0.6513	0.00983
Hdac1	0.414	0.0105	*Hdac1*	0.42008	0.01231
Smarca4	0.54283	0.01004	*Smarca4*	0.44926	0.00316
Myc	0.76267	0.01689	*Smarca2*	0.76184	0.00033
Smarca2	0.90388	3.21E-07	*Nr2f2*	0.97183	0.00019
Gata2	1.04024	0.00051	*Myc*	1.0391	9.00E-06
Tcf7l1	1.04887	0.0004	*Tbx5*	1.14632	4.25E-07
Foxc1	1.15313	0.00019	*Gata2*	1.16332	0.00088
Nppa	1.20529	9.57E-17	*Tcf7l1*	1.25224	3.58E-09
Tbx5	1.35936	3.59E-15	*Gata3*	1.29114	0.00742
Nr2f2	1.58927	1.98E-17	*Foxc1*	1.29823	2.09E-08
Foxc2	1.74901	3.82E-05	*Tbx2*	1.40012	1.07E-05
Rarg	2.02173	7.08E-07	*Rarg*	1.44205	1.67E-05
Gata3	2.04706	1.20E-09	*Nppa*	1.65797	0.00218
Shox2	2.19626	0.00187	*Foxc2*	2.13984	3.36E-09
Tbx2	2.41087	1.46E-05	*Shox2*	2.69182	3.94E-18
Isl1	4.09134	1.58E-10	*Hoxa3*	2.7783	0.0006
Hoxa3	4.15614	1.96E-09	*Isl1*	2.93557	1.61E-08

Scale
1
2
3
4
5
6
7
8
9
10

Differentially-expressed genes in the right atrium of naïve *Ahr*$^{-/-}$ and ligand-exposed *Ahr*$^{+/+}$ at E15.5. Magnitude of change (log ratio) and p-values are color-coded from lower (blue) to higher (red) values.

b. Supplemental Table S2

Nkx2-5 mutant gene expression (*Prall et al 2007)*	***Ahr*$^{+/+}$ + TCDD**		***Naïve Ahr*$^{-/-}$**	
Downregulated	**Direction**	**Agrees Nkx2-5 mutant**	**Direction**	**Agrees Nkx2-5 mutant**
Ankrd1	up	no	unchanged	no
Nppb (Bnp)	down	yes	down	yes
Nr2f2 (coup TFII)	up	no	up	no
Myl2	down	yes	down	yes
Irx4	down	yes	down	yes
Smpx (Chisel)	unchanged	no	down	yes
Nppa (Anf)	up	no	up	no
Wnt11	up	no	up	no
Upregulated				
IGFBP5	up	yes	up	yes
Pdgfra	up	yes	up	yes
Tnc	up	yes	up	yes
Isl1	up	yes	up	yes
Tbx5	up	yes	up	yes
Bmp2	unchanged	no	unchanged	no
Fgf10	up	yes	up	yes
Hhex	unchanged	no	unchanged	no
Unaltered				
Cer1	unchanged	yes	unchanged	yes
Dan	unchanged	yes	unchanged	yes
NOG	unchanged	yes	unchanged	yes
Bmp4	up	no	up	no
Bmp7	down	no	down	no
Dkk1	unchanged	yes	unchanged	yes

Comparative analysis of the differentially-expressed genes in the right atrium of naïve *Ahr*$^{-/-}$ and ligand-exposed *Ahr*$^{+/+}$ at E15.5 with the previously-published cardiac transcriptome of *Nkx2-5* mutant mice (Prall et al. 2007). Similarities in identity and direction of change are highlighted in yellow.

4. Supplemental Figures

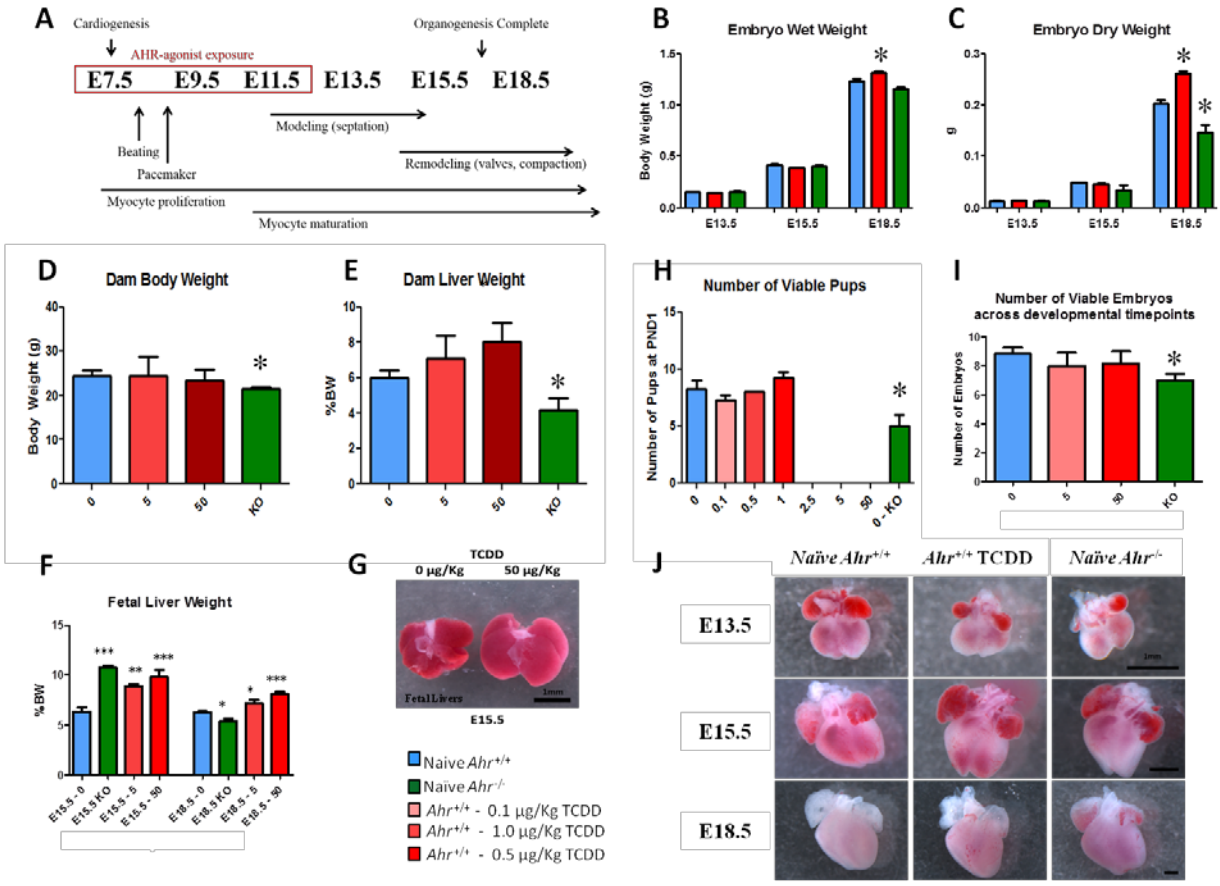

a. Supplemental Figure S1 - (A) Experimental design for gestational exposure to the prototypical AHR ligand (TCDD). (B) Whole embryo wet weight (grams) from naïve *Ahr*$^{+/+}$, ligand-exposed *Ahr*$^{+/+}$, and *Ahr*$^{-/-}$ embryos at the indicated developmental timepoints. Mean ± SEM; * p≤0.05. (C) Whole embryo dry weight (grams) from naïve *Ahr*$^{+/+}$, ligand-exposed *Ahr*$^{+/+}$, and *Ahr*$^{-/-}$ embryos at the indicated developmental timepoints. Mean ± SEM; * p≤0.05. (D) Maternal body weight (grams) from naïve *Ahr*$^{+/+}$dams, *Ahr*$^{+/+}$dams exposed to 5 or 50 µg/kg of AHR ligand (TCDD), and *Ahr*$^{-/-}$ dams. Mean ± SEM; * p≤0.05. (E) Maternal liver weight (expressed as the percent of body weight) from naïve *Ahr*$^{+/+}$dams, *Ahr*$^{+/+}$dams exposed to 5 µg/kg or 50 µg/kg of AHR ligand (TCDD), and *Ahr*$^{-/-}$ dams. Mean ± SEM; * p≤0.05. (F) Fetal liver weight (expressed as the percent of body weight) from naïve *Ahr*$^{+/+}$, ligand-exposed *Ahr*$^{+/+}$, and *Ahr*$^{-/-}$ embryos at the indicated developmental timepoints. Mean ± SEM; * p≤0.05. (G) Representative macroscopic illustration of AHR ligand-induced fetal liver enlargement. Scale bar = 1mm. (H) Pup viability (i.e. pups alive at 24 hours postpartum) from naïve *Ahr*$^{+/+}$dams, *Ahr*$^{+/+}$dams exposed to 0.1, 5, or 50 µg/kg of AHR ligand (TCDD), and *Ahr*$^{-/-}$ dams. Mean ± SEM; * p≤0.05. (I) Embryo viability (i.e. live embryos at E13.5, E15.5 or E18.5) from naïve *Ahr*$^{+/+}$dams, *Ahr*$^{+/+}$dams exposed to 5 or 50 µg/kg of AHR ligand (TCDD), and *Ahr*$^{-/-}$ dams. Mean ± SEM; * p≤0.05. (J) Representative macroscopic illustration of embryo hearts from naïve *Ahr*$^{+/+}$, ligand-exposed *Ahr*$^{+/+}$, and *Ahr*$^{-/-}$ embryos at E13.5, E15.5, and E18.5. Scale bar= 1mm.

Naïve *Ahr*$^{+/+}$ Naïve *Ahr*$^{-/-}$ *Ahr*$^{+/+}$ + TCDD

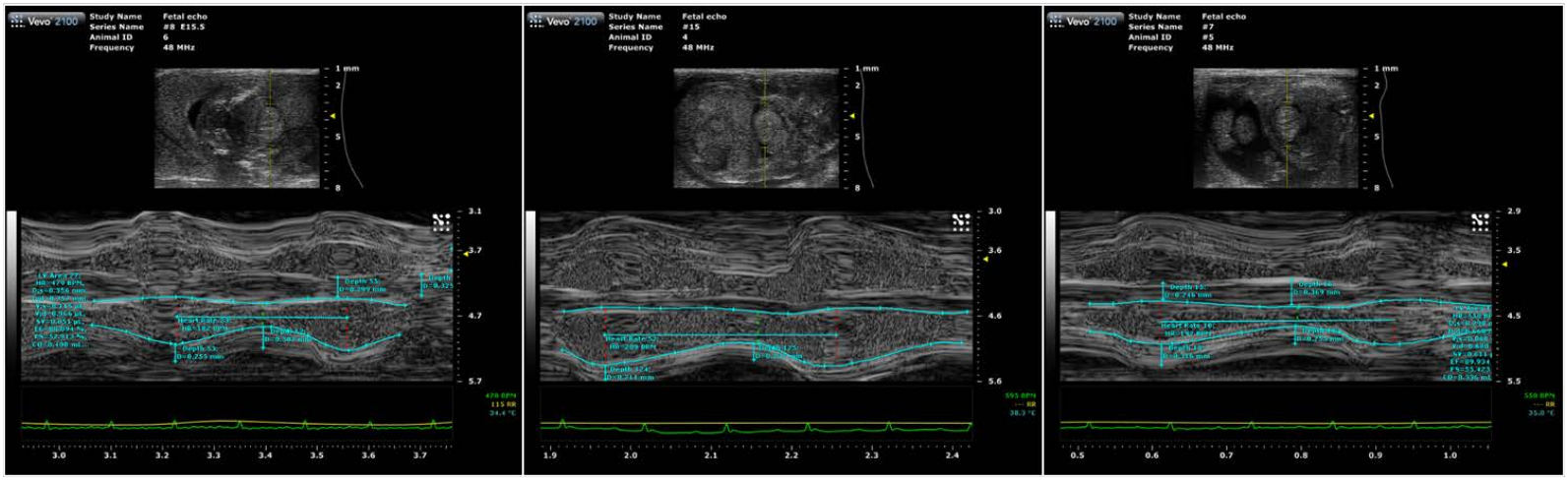

b. Supplemental Figure S2 – Annotated representative *in utero* echocardiography illustrations at E15.5 from *Ahr*$^{+/+}$, naïve or exposed to AHR ligand (TCDD) *in utero*, and *Ahr*$^{-/-}$ embryos.

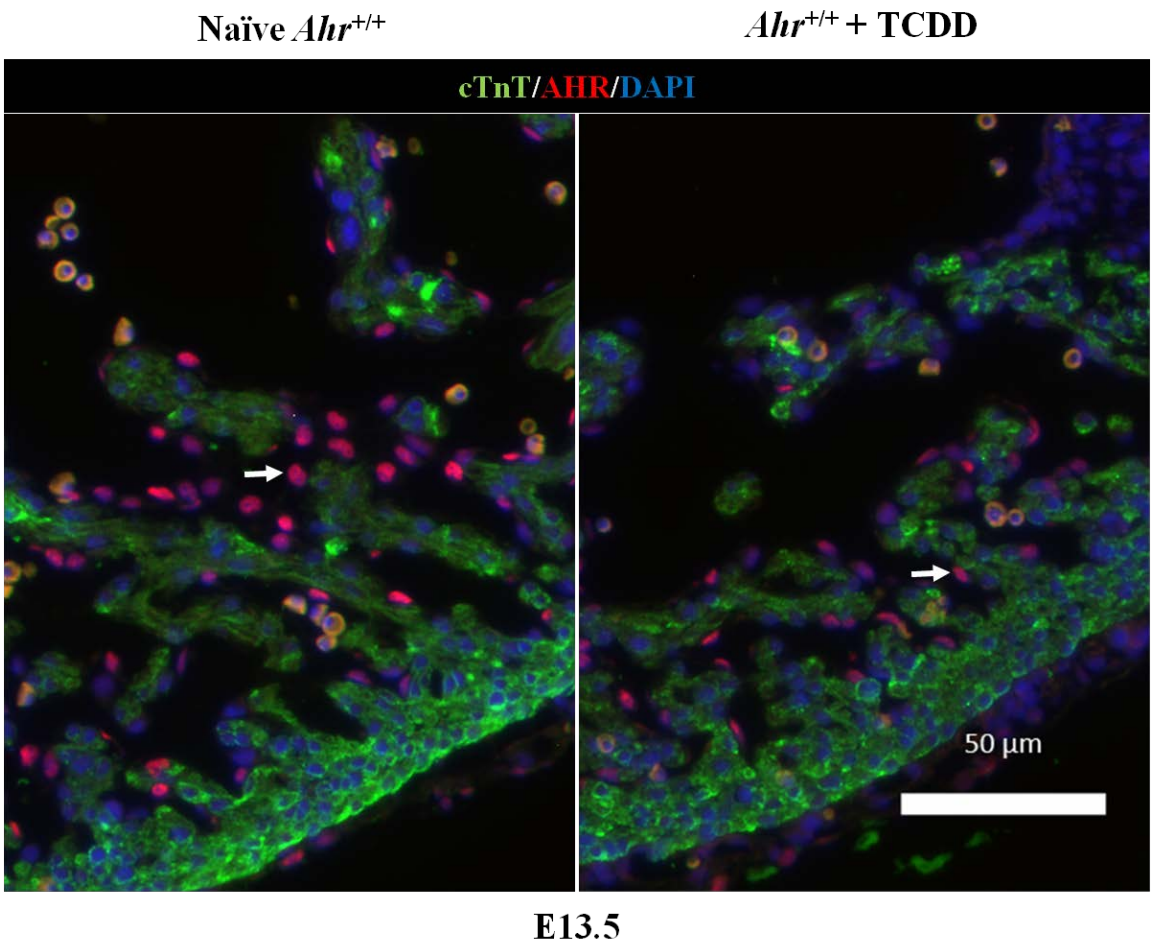

c. Supplemental Figure S3 - Five-micron sections of embryonic hearts collected at E13.5 from *Ahr*$^{+/+}$, naïve or exposed to AHR ligand (TCDD) *in utero*, were used for immunofluorescent detection of AHR (red) and cardiac troponin T (green). Staining with DAPI identifies the nuclei. AHR – aryl hydrocarbon receptor, cTnT – cardiac troponin T, DAPI – nuclei, scale bar = 50 µm.

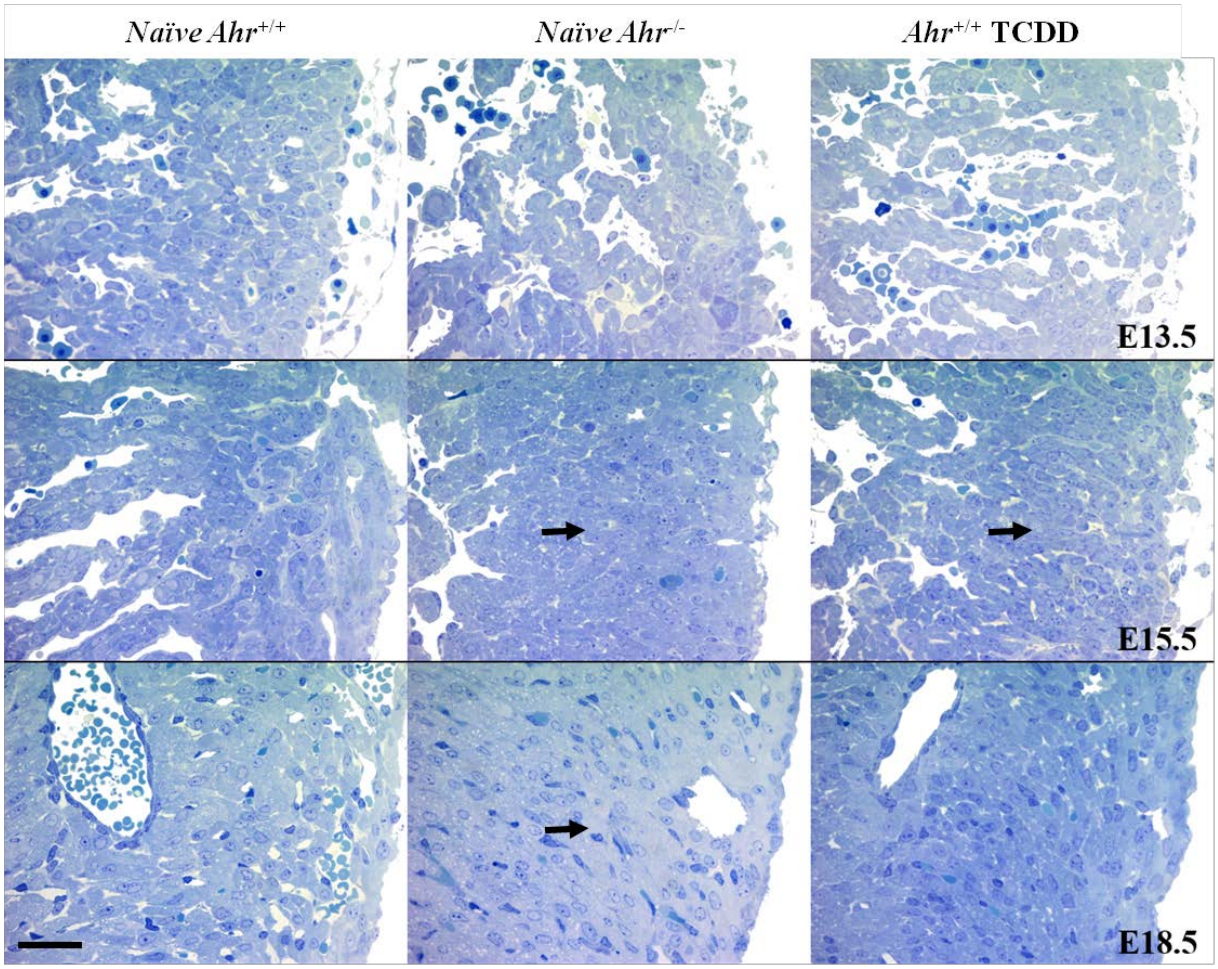

d. Supplemental Figure S4 - One-micron sections of embryonic hearts collected at E13.5, E15.5, and E18.5 from *Ahr*$^{+/+}$, naïve or exposed to AHR ligand (TCDD) *in utero*, and *Ahr*$^{-/-}$ hearts were used for histomorphometric assessment of the developing myocardium. The compact myocardium is identified by the arrows. Toluidine blue stain, scale bar = 100 µm.

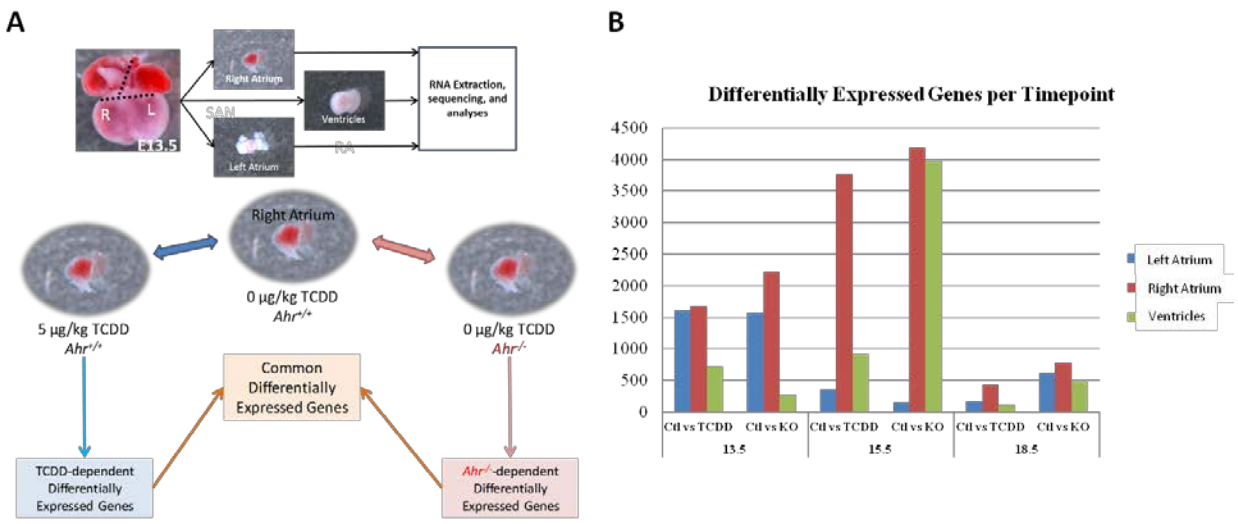

e. Supplemental Figure S5 - (A) Experimental design for RNA.seq experiment and analyses. RNA sequencing of naïve *Ahr*$^{+/+}$, *Ahr*$^{-/-}$, and ligand-exposed *Ahr*$^{+/+}$ embryonic hearts. Hearts were microdissected into right atrium, left atrium, and ventricles, at the three distinct developmental milestones in cardiogenesis (E13.5, E15.5, and E18.5). An example comparison for E13.5 heart and right atrium compartment is shown. (B) Differentially expressed genes from naïve *Ahr*$^{+/+}$, ligand-exposed *Ahr*$^{+/+}$, and *Ahr*$^{-/-}$ embryo hearts at the indicated developmental timepoints.

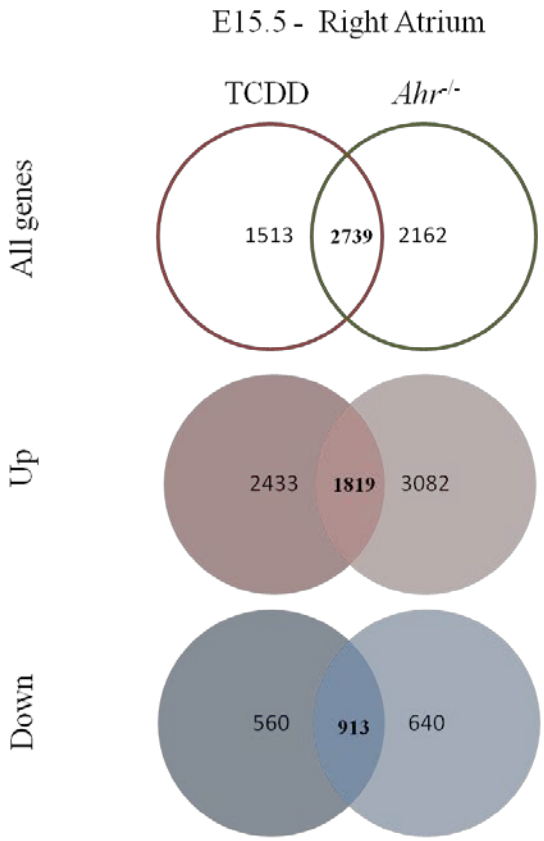

f. Supplemental Figure S6 - Venn diagrams illustrating the number of commonly differentially-expressed genes in the right atrium at E15.5 of *Ahr*$^{-/-}$ and ligand-exposed *Ahr*$^{+/+}$ embryonic hearts, relative to naïve *Ahr*$^{+/+}$.

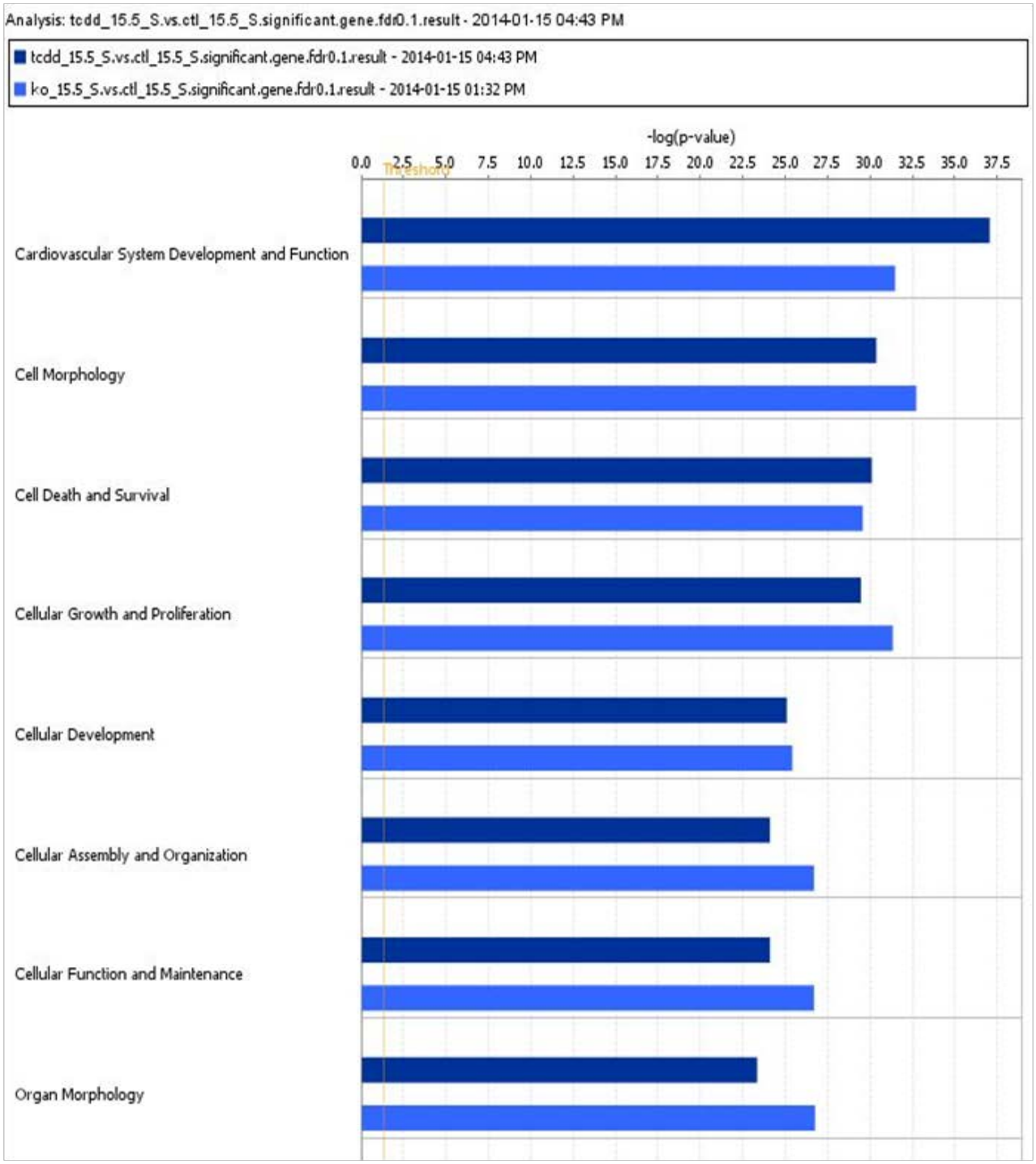

g. Supplemental Figure S7 - Differentially-expressed Ingenuity® IPA's networks.

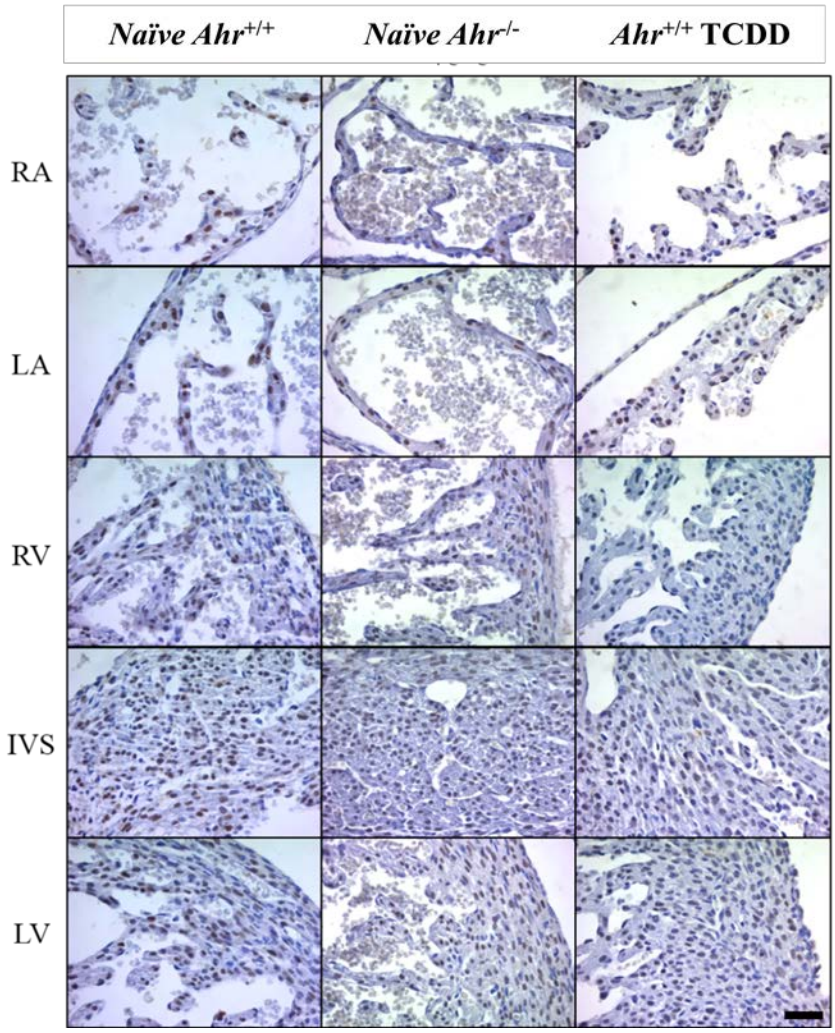

h. Supplemental Figure S8 - (A) Five-micron sections of embryonic hearts collected at E13.5, E15.5, and E18.5 across subanatomical areas (RA, right atrium; LA, left atrium; RV, right ventricle; IVS, interventricular septum; LV, left ventricle) from *Ahr*$^{-/-}$ and *Ahr*$^{+/+}$ either naïve or exposed to TCDD *in utero*, were used for immunohistochemical detection of NKX2-5 and counterstained with Harris hematoxylin. Scale bar = 50 µm.

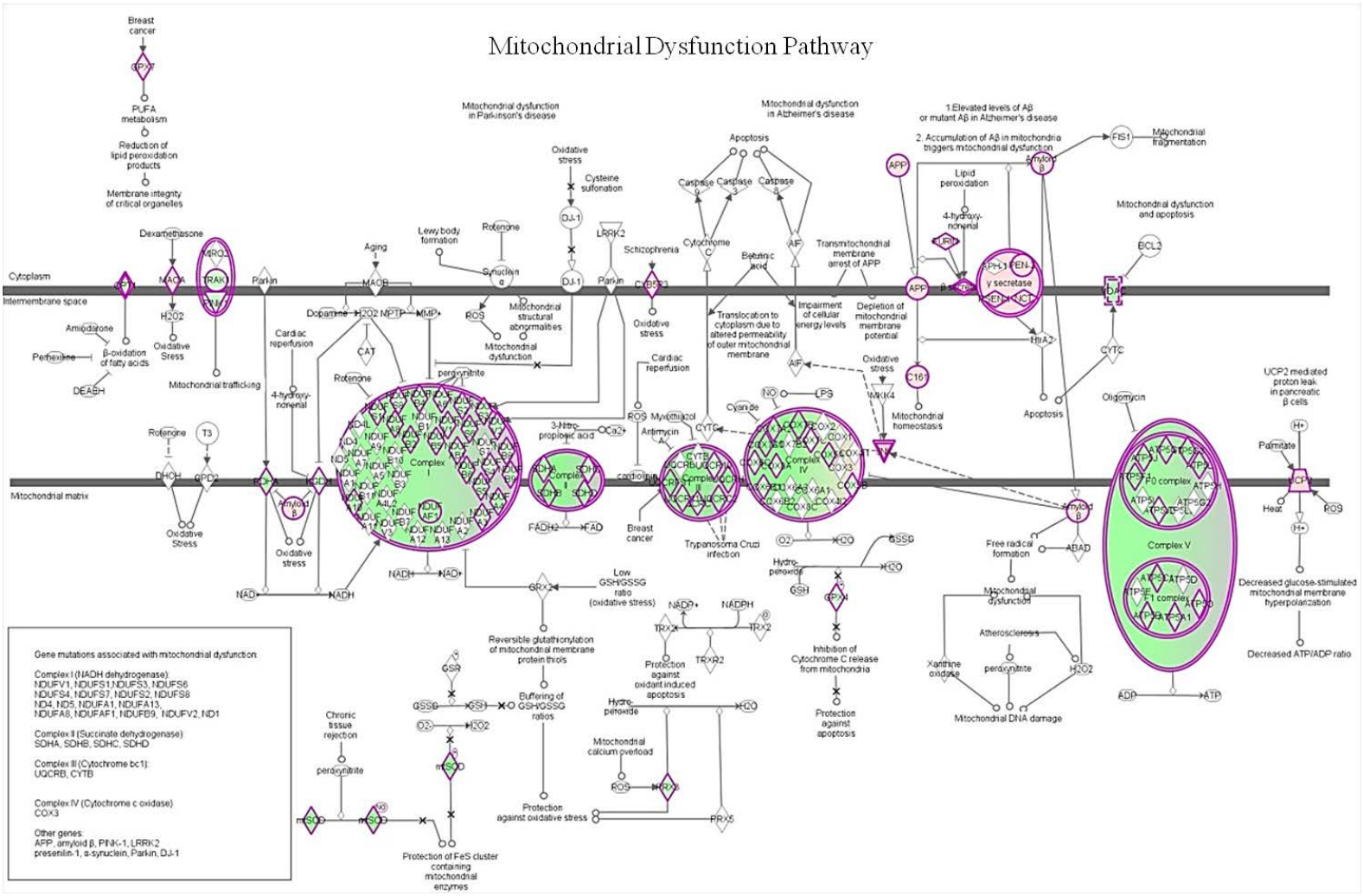

i. Supplemental Figure S9 - Ingenuity® IPA Mitochondrial Dysfunction Pathway status at E.15.5 in the right atrium of ligand-exposed *Ahr*$^{+/+}$ embryo hearts relative to naïve *Ahr*$^{+/+}$ embryo hearts. Magenta lines indicate nodes with differentially-expressed genes. Shades of green indicate downregulation while shades of red indicate upregulation; blank nodes indicate no differential expression.

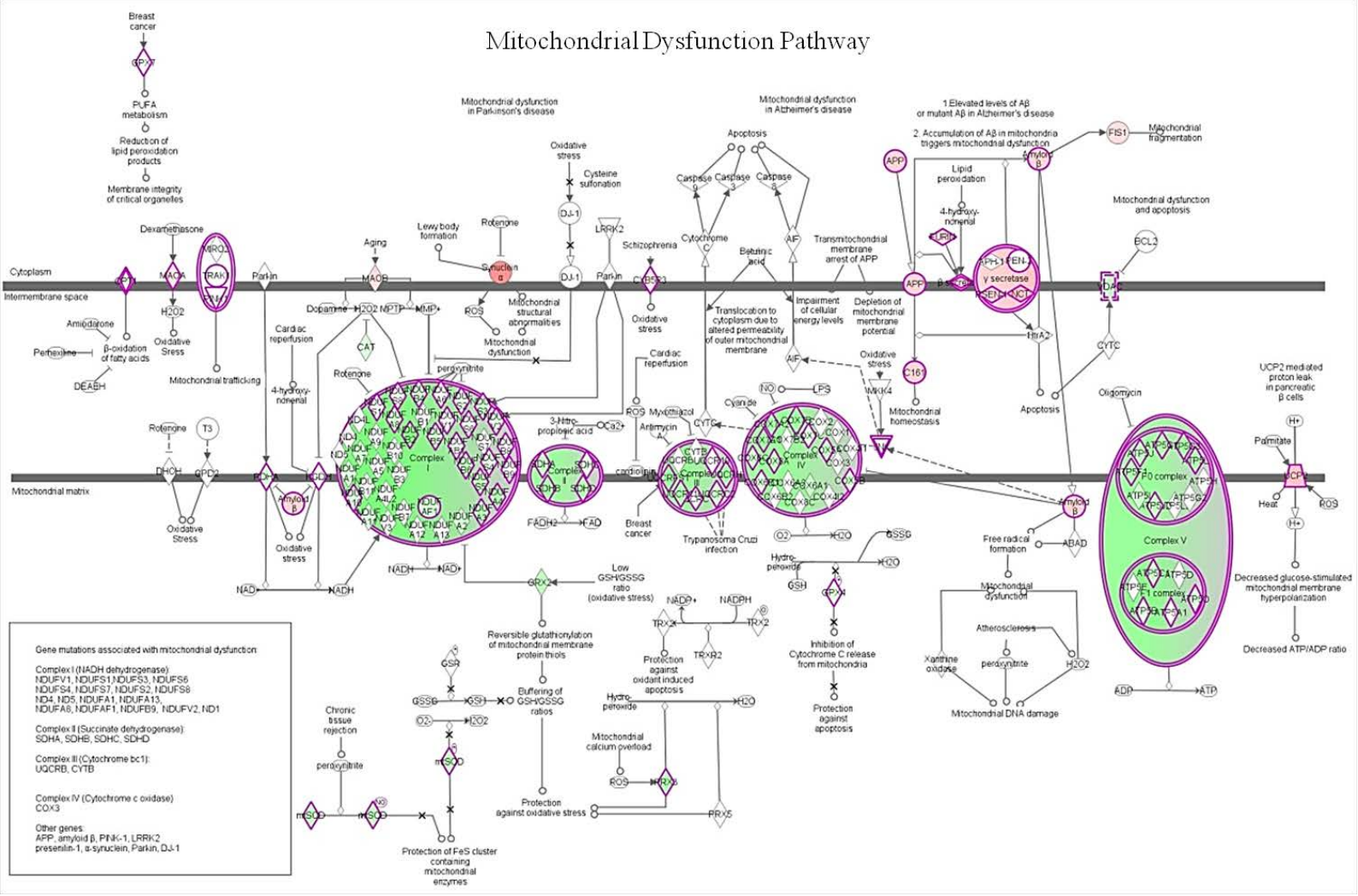

j. Supplemental Figure S10 - Ingenuity® IPA Mitochondrial Dysfunction Pathway status at E.15.5 in the right atrium of ligand-exposed *Ahr*$^{-/-}$ embryo hearts relative to naïve *Ahr*$^{+/+}$ embryo hearts. Magenta lines indicate nodes with differentially-expressed genes. Shades of green indicate downregulation while shades of red indicate upregulation; blank nodes indicate no differential expression.

Supplemental References

Abbott BD, Schmid JE, Pitt JA, Buckalew AR, Wood CR, Held GA, Diliberto JJ. 1999. Adverse reproductive outcomes in the transgenic Ah receptor-deficient mouse. *Toxicol Appl Pharmacol* **155**: 62–70.

Besteman EG, Zimmerman KL, Huckle WR, Prater MR, Gogal RM, Holladay SD. 2007. 2,3,7,8-tetrachlorodibenzo-p-dioxin (TCDD) or diethylstilbestrol (DES) cause similar hematopoietic hypocellularity and hepatocellular changes in murine fetal liver, but differentially affect gene expression. *Toxicol Pathol* **35**: 788–94.

DeVito MJ, Birnbaum LS, Farland WH, Gasiewicz TA. 1995. Comparisons of estimated human body burdens of dioxinlike chemicals and TCDD body burdens in experimentally exposed animals. *Environ Health Perspect* **103**: 820–31.

Lahvis G, Lindell S, Thomas R, McCuskey R, Murphy C, Glover E, Bentz M, Southard J, Bradfield C. 2000. Portosystemic shunting and persistent fetal vascular structures in aryl hydrocarbon receptor-deficient mice. *Proc Natl Acad Sci USA* **97**: 10442–10447.

Teekakirikul P, Eminaga S, Toka O, Alcalai R, Wang L, Wakimoto H, Nayor M, Konno T, Gorham JM, Wolf CM, et al. 2010. Cardiac fibrosis in mice with hypertrophic cardiomyopathy is mediated by non-myocyte proliferation and requires Tgf-β. *J Clin Invest* **120**: 3520–9.

Weinstein DA, Gogal RM, Mustafa A, Prater MR, Holladay SD. 2008. Mid-gestation exposure of C57BL/6 mice to 2,3,7,8-tetrachlorodibenzo-p-dioxin causes postnatal morphologic changes in the spleen and liver. *Toxicol Pathol* **36**: 705–13.